PCCP

PAPER

View Article Online
View Journal | View Issue

Cite this: *Phys. Chem. Chem. Phys.*, 2016, **18**, 28281

Incorporating QM and solvation into docking for applications to GPCR targets†

Minsup Kim and Art E. Cho*

Received 7th July 2016,
Accepted 9th September 2016

DOI: 10.1039/c6cp04742d

www.rsc.org/pccp

A great number of GPCR crystal structures have been solved in recent years, enabling GPCR-targeted drug discovery using structure-based approaches such as docking. GPCRs generally have wide and open entrances to the binding sites, which render the binding sites readily accessible to solvent. GPCRs are also populated with hydrophilic residues in the extracellular regions. Thus, including solvent and polarization effects can be important for accurate GPCR docking. To test this hypothesis, a new docking protocol which incorporates quantum mechanical/molecular mechanical (QM/MM) calculations along with an implicit solvent model is developed. The new docking method treats the ligands and the protein residues in the binding sites as QM regions and performs QM/MM calculations with implicit solvent. The results of a test on all solved GPCR cocrystals show a significant improvement over the conventional docking method.

Introduction

G protein-coupled receptors (GPCRs) are promising targets in the field of drug discovery. They form a large and diverse family of proteins and exist in nearly 800 members of the mammal class.[1] In human bodies, GPCRs function in every organ system and play the role of cell surface signaling proteins in many physiological processes. For this reason GPCRs have connections to a number of human diseases such as cancer, central nervous system disorders, cardiac dysfunction, diabetes, obesity, inflammation and pain.[2] These ubiquitous and disease-related characteristics of GPCRs offer quite a few opportunities to develop novel drugs.[3] At present, GPCR targeted drugs are, in fact, one of the best selling drugs on the market encompassing 26% of FDA approved drugs and with a market share of 40% of all pharmaceuticals prescribed. Clarinex (Schering-Plough), Zyprexa (Eli Lilly), Neurontin (Pfizer), Cozaar (Merck & Co), Zantac (GlaxoSmithKline), and Zelnorm (Novartis) are prominent examples of drugs that act on GPCRs.[2,4]

Even though GPCRs present many possibilities in the field of drug development, only a few GPCR members have been exploited as targets of the current drugs.[5] Until just a few years ago, lack of high resolution atomic structures of GPCRs had been the biggest hurdle to structure-based drug design (SBDD) targeting GPCRs. However, the problem has been alleviated by the Nobel-prize-winning work of Lefkowitz and Kobilka, which triggered a flood of new solved GPCR structures. On the other hand, significant advance has also been made in the field of GPCR structure prediction, which was evident in recent GPCR modeling competition.[6]

With a growing body of solved GPCR structures, structure-based drug design is now viable for GPCR targets.[7] In SBDD, one utilizes structural information of target proteins by employing computational methods.[8] Docking is one of the main computational methods used in SBDD. It allows researchers to screen a library of compounds virtually by predicting binding modes and affinities and thereby save time and cost of synthesizing in an effort to obtain lead compounds.[9]

However, the current docking programs can exhibit some problems when applied to GPCRs. According to a recent GPCR docking assessment report[10] using a commonly used docking program Glide, several GPCRs can pose problems even though the success rate was over 70%. For adenosine A_{2A}, ZM241385 and XAC, which have flexible solvent exposed groups, Glide could not find correct binding poses. The docking errors for A_{2A} have been addressed and solved using an induced fit docking or binding site water molecule inclusion strategy,[11] but these solutions are not universally applicable. Induced fit docking showed slight improvements of about 0.1 Å in average RMSD on the set of GPCRs, but the success rate was not improved.

Allosteric modulators of GPCR have advantages over orthosteric drugs for their selectivity and reduced toxicity potential and have been attracting more attention in recent years.[12] However, since allosteric binding sites tend to be more solvent exposed than their orthesteric counterparts, it is not clear if the current docking practice would work well for them.[13]

In an attempt to develop a docking method that can predict accurate binding poses universally for GPCR targets, we first analyze the binding sites of GPCRS and reflect the results of the analysis in a new docking protocol. In this paper, we first describe a process in which structural features of GPCR binding sites are identified. A new docking protocol which attends to

Department of Bioinformatics, Korea University, Sejong, 339-700, Korea. E-mail: artcho@korea.ac.kr

† Electronic supplementary information (ESI) available. See DOI: 10.1039/c6cp04742d

these features and involves QM/MM calculations and the solvent effect is then presented. Finally, we show how this new docking protocol can achieve high accuracy in docking pose prediction through comparison tests on GPCR cocrystals.

Methods

GPCR docking assessment set

The GPCR docking assessment set used for our tests comprises all atomic structures of GPCR–ligand complexes solved by 2013 (Table 1). The structures collected from the RCSB Protein Data Bank website (http://www.rcsb.org) were: Beta2 adrenergic receptor, Beta1 Adrenergic receptor, Alpha2 Adenosine receptor, Dopamine Receptor 3, Histamine receptor 1, M3 muscarinic acetylcholine receptor, opioid receptor, Nociceptin/orphanin FQ receptor, protease-activated receptor 1, M2 muscarinic acetylcholine receptor, Sphingosine 1-phosphate receptor, corticotropin-releasing factor receptor 1, smoothened receptor, 5-hydroxytryptamine receptor and CCR5 Chemokine receptor families. Rhodopsin receptors and several GPCRs that have covalent bonds with ligands or invalid structures in binding

Table 1 GPCR docking assessment set

GPCR	PDB	Ligand
Human beta2-adrenergic-aceptor (β2AR)	2RH1	Carazolol
	3D4S	Timolol
	3NY8	ICI118551
	3NY9	Compound#1
	3NYA	Alprenolol
	3SN6	BI-167107
	4LDL	Hydroxybenzyl isoproterenol
	4LDO	Adrenaline
Turkey beta1-adrenergic-aceptor (β1AR)	2VT4	Cyanopindolol
	2Y00	Dobutamine
	2Y02	Carmoterol
	2Y03	Isoprenaline
	2Y04	Salbutamol
	2YCW	Carazolol
	4AMI	Bucindolol
	3ZPQ	Arylpiperazine
	4AMJ	Carvedilol
Human alpha2 adenosine receptor ($A_{2A}R$)	3EML	ZM241385
	2YDO	Adenosine
	2YDV	NECA
	3REY	XAC
	3RFM	Caffeine
	3UZA	4g
	3UZC	4e
Human dopamine receptor 3 (D_3R)	3PBL	Eticlopride
Human histamine receptor 1 (H_1R)	3RZE	Doxepin
Human M3 muscarinic acetylcholine receptor (CHRM3)	4DAJ	Tiotropium
Human opioid receptor (OPRK1)	4DJH	JDTic
	4EJ4	Naltrindole
Human nociceptin/orphanin FQ receptor (KOR3)	4EA3	C-24
Human protease-activated receptor 1 (PAR1)	3VW7	Vorapaxar
Human M2 muscarinic acetylcholine receptor (CHRM2)	3UON	QNB
	4MQS	Iperoxo
	4MQT	LY2119620
Sphingosine 1-phosphate receptor ($S1P_1$)	3V2W	ML056
Human corticotropin-releasing factor receptor 1 (CRF_1R)	4K5Y	CP-376395
Human smoothened receptor (SMO)	4JKV	LY2940680
5-Hydroxytryptamine (5-HT) receptor	4IAR	Ergotamine
	4IAQ	Dihydroergotamine
CCR5 chemokine receptor (CCR5)	4MBS	Maraviroc

sites were excluded from the assessment set. It has been reported that ConfGen,[14] the conformational search algorithm in Glide cannot generate bioactive conformations for UK-432097 and IT1t,[10] so their complexes 3QAK and 3ODU were excluded from the docking assessment set. In the case of multiple entries of the same co-crystals in the PDB, we selected only one from each group of overlapping complex structures. All the collected structures were treated with the Protein Preparation Wizard module[15] of the Schrödinger suite for docking. The module assigns correct bond orders and adds hydrogens based on Epik calculations for appropriate pK_a values.[16] Protein Assignment utility[17] of the module resolved the structural ambiguities of the crystal structure, including protonation states and tautomers of His residues, "flip" assignments for Asn, Gln and His residues and protonation states of Asp, Glu, Tyr and Lys residues. Heterogen (HET) molecules except for native ligands were eliminated and missing side chains were filled and their orientations were optimized by Prime.[18] Restrained minimization was performed to relax only the added hydrogens using Impact[19] with OPLS 2005 force field.

Docking method

All the dockings in this research were performed using Glide 5.7.[20,21] Glide generates ligand poses, puts them through a series of hierarchical filters, and evaluates them using a scoring function, which contains both energy-based and empirical functions. In our calculations, we first kept 5000 poses per ligands from initially generated conformations for the refinement. After the refinement we kept 400 poses for energy minimization using grids and ranked them using a scoring function called GlideScore. In Glide, ligand charges are assigned using OPLS 2005 force field partial charges. We used the SP (standard precision) mode of Glide and allowed flexible ligand sampling.

Solvation scoring method

To consider the solvation effect in docking, we used the Embrace module of MacroModel.[22] Embrace calculates ligand–receptor binding energies by molecular mechanics of the complex and the separated receptor and ligand using the GB/SA continuum solvation model. Before applying this method to ligand–receptor complexes, we first performed docking and produced various ligand conformations. We generated 10 000 initial poses in the initial phase of docking using Glide and clustered them by a RMSD of 1.5 Å. Eventually, we prepared 10 possible ligand poses for each ligand. After the clustering we scored and ranked the representative poses using Embrace. The Embrace calculations were run in an energy difference mode. In this mode, energies of receptors, ligands and complexes are computed separately with OPLS 2005 force field in a solvent environment and the energy difference is then calculated using the equation ($\Delta E = E_{complex} - E_{ligand} - E_{protein}$). The full effect of solvation is included in this mode. Top ranked poses by ΔE were selected as the final predictions.

QM/MM docking protocols

Our QM/MM docking protocol is akin to the early QM/MM docking method developed in the previous research, which uses calculated partial charges by QM/MM for docking instead of fixed force field charges.[23] Our protocol begins with QM/MM calculations. For QM/MM, we employed QSite,[24] which combines Jaguar[25] for the QM region and Impact[19] for the MM region. QSite is based on the additive scheme,[26–28] in which coupling between MM and QM regions is modelled by electrostatic embedding. For a "cut" of a bond between MM and QM regions it uses the frozen orbital method.[24] We defined ligands and the surrounding receptor region including the side chains within 5 Å of the ligand as the QM region and all others as the MM region. For the QM region, density functional theory (DFT) was used with the B3LYP hybrid functional and the 6-31G** basis set. OPLS 2005 force field was used for MM calculations. After QM/MM calculations, we calculated partial charges of the atoms in the QM regions using electrostatic potential (ESP) fitting. In the case of solvation QM/MM docking, we used the Poisson Boltzmann (PB) Solver to add the solvation effect in QM/MM calculations. In this implicit solvent model, QSite first calculates the ESP charges for QM regions in the gas phase and passes them to the PB solver, which in turn refits the charges to the field produced by the solvent dielectric continuum. This iterative process would be continued until the solvation free energy for the molecule converges. In our calculations, the iteration was terminated when the change in energy is less than 5×10^{-5} hartree. In the ESI,† S1, we summarized the convergence characteristic in the solvation QM/MM charge calculations. After partial charge calculations, we substituted the charge values in the structure files for ligands and receptors with these values and forced Glide to use them in the re-docking calculations.

Practical solvation QM/MM docking protocol

In order to apply the solvation QM/MM docking protocol in an actual industry setting, in which knowledge of native ligand pose is absent, we incorporated the SOF (survival of the fittest) algorithm,[23] which was introduced in an earlier version of the QM/MM docking protocol developed in our laboratory. In this protocol, since native ligand poses are not available for a real target, we first generate up to 10 poses with regular Glide SP then perform QM/MM based atomic charge fitting on each of these poses. With these new sets of atomic charges, we carry out subsequent rounds of docking calculations. From the resulting pose predictions, we select the best pose based on electrostatic-van der Waals energies.

Results

Re-docking test using a conventional docking program

We first carried out re-docking tests on the GPCR docking assessment set, in which one docks the co-crystal ligand back to the receptors and compares the predictions with the crystal structures, in order to confirm how well a conventional docking program performs on GPCRs. Listed in Table 2 are RMSD (root-mean-square deviation of atom positions) values of the re-docking results. Usually in docking tests, 2 Å RMSD is widely

used as a criterion for a successful docking. In the same criterion, Glide succeeded in predicting ligand binding poses in 32 of 40 cases, with 27 cases being under 1 Å. However, RMSD's of the failed cases are rather high being in the range of 2.33–9.66 Å. In the cases of 4AMI, 3EML, 3UZA and 3PBL, the RMSD values were over 5 Å, which means that the predicted ligand binding poses were in either completely wrong orientations or in wrong positions. Furthermore, Glide did not show consistent docking results for the same receptors with different ligands in some cases. In particular, for $A_{2A}R$, RMSD with NECA was 0.254 Å and with ZM241385 was 8.976 Å. Another example is β1AR, in which bucindolol showed the worst result (9.661 Å) in our re-docking tests while the other ligands were successes. Further analysis is needed to decipher the reasons behind these failures of the current docking practice in order to improve docking methods for GPCRs.

A cause of docking failures in GPCRs

Docking processes can be divided into 'searching' and 'scoring' steps. In our re-docking tests, we observed that the search algorithm generated at least one accurate ligand pose (RMSD under 2 Å) to all GPCR test sets (data not shown), but the scoring function could not pick the correct pose as the best scored one in the failed cases. In search of a possible cause of the problem, we focused on the fact that ligands of failed cases commonly have solvent exposed parts in crystals (Fig. 1).

Since Glide does not take into account the solvent effect, a solvent exposed region of ligands can be a factor that hinders accurate dockings. Inspection of the re-docking results in detail reveals that this is indeed the case. Among the ligands for A_{2A}, Glide could predict correct binding poses for Adenosine, NECA and T4E, which do not have solvent exposed parts, whereas it could not for ZM241385 and XAC, which do have solvent

Table 2 RMSD values (Å) of re-docking on GPCRs using the five docking methods (Glide, Solvation rescoring, QM/MM docking, solvation QM/MM docking and gas phase QM docking)

	Glide SP docking	Solvation scoring	QM/MM docking	solvation QM/MM docking	Gas phase QM docking
PDB	RMSD (Å)	RMSD (Å)	RMSD (Å)	RMSD (Å)	RMSD (Å)
2RH1	0.890	0.758	0.847	0.858	0.746
3D4S	0.835	1.016	0.559	0.563	0.899
3NY8	0.895	1.018	1.227	0.568	2.735
3NY9	0.762	0.923	0.878	0.802	0.807
3NYA	0.672	0.680	0.723	0.557	1.138
3SN6	1.428	1.461	1.398	1.414	1.886
4LDL	1.458	0.442	0.467	0.406	0.456
4LDO	0.826	0.750	1.328	0.721	0.754
2VT4	0.619	0.507	0.682	0.649	0.526
2Y00	0.722	0.720	0.714	0.709	1.657
2Y02	0.380	1.699	1.108	1.108	0.714
2Y03	0.619	1.917	0.511	0.589	0.736
2Y04	0.509	0.509	0.370	0.383	0.528
2YCW	0.533	0.534	0.693	0.614	0.429
4AMI	9.661	2.914	2.924	0.489	9.277
3ZPQ	0.413	0.413	0.743	0.662	0.412
4AMJ	0.962	1.758	0.624	1.507	1.371
3EML	8.976	6.275	6.355	0.546	8.810
2YDO	0.641	0.934	0.504	0.508	0.624
2YDV	0.254	0.317	0.289	0.309	0.208
3REY	3.520	4.012	3.996	1.223	1.120
3RFM	3.079	4.054	0.812	0.805	4.581
3UZA	5.946	5.926	0.983	0.989	3.877
3UZC	1.679	1.698	1.914	1.962	0.440
3PBL	7.264	7.252	1.403	1.393	7.237
3RZE	0.666	0.662	0.420	0.416	0.778
4DAJ	1.261	0.916	0.914	1.271	0.942
4DJH	5.339	5.357	0.934	0.893	2.032
4EJ4	0.722	0.715	0.735	0.730	0.933
4EA3	1.410	1.191	1.342	1.118	2.569
3VW7	0.497	0.579	1.477	1.051	1.318
3UON	0.587	0.609	0.586	0.593	0.565
4MQS	0.423	0.423	0.304	0.342	0.640
4MQT	2.334	5.421	3.100	1.507	2.254
3V2W	0.763	0.579	0.838	0.922	1.035
4K5Y	0.478	0.478	0.325	0.325	0.355
4JKV	0.378	0.358	0.493	0.500	0.423
4IAR	0.408	0.331	0.429	0.411	0.402
4IAQ	0.297	0.293	0.279	0.272	0.340
4MBS	0.297	0.306	0.373	0.363	0.342
Average	1.735	1.668	1.115	0.776	1.672
Range	0.254–9.661	0.293–7.252	0.279–6.355	0.272–1.962	0.208–9.277
Success rate	32/40	32/40	36/40	40/40	31/40

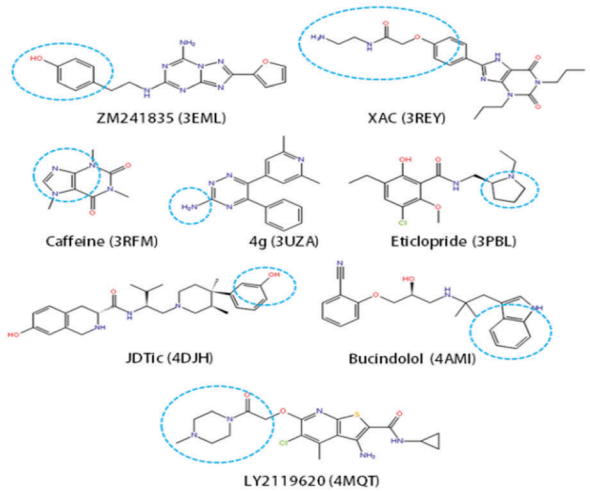

Fig. 1 Solvent exposed ligands in GPCR crystals. The corresponding PDB code and ligand name are shown under each ligand. Solvent exposed parts of ligands are marked with blue dotted circles.

exposed parts. Among β1AR ligands, bucindolol is the only one with solvent exposed parts and also the only one for which Glide failed to predict the correct binding pose.

To understand the way in which the ligands have solvent exposed parts in the GPCR binding site, we analyzed two A_{2A} adenosine receptor co-crystals in complex with caffeine and ZM241385. In the binding pose of ZM241385, the solvent exposed phenol group is located at the entrance of the binding site where the binding site and the extracellular solvents are in contact (Fig. 2A). In the binding pose of caffeine, although the whole ligand is located in the deep binding site (Fig. 2B), it is still partially exposed to solvents. The latter case of caffeine shows that the extracellular solvents can access the deeper part of the binding site even though it is located inside the membrane region. These 2 examples illustrate the fact that the A_{2A} adenosine receptor has a wide and open binding site, which is readily accessible by water molecules from the extracellular region. Adenosine, NECA and T4E are exceptions since they are not only wedged in the deeper part of the binding site but also protected from solvents by an extracellular loop that went through conformational change by the induced fit effect.

This feature is not unique to $A_{2A}R$ and attributed to the general 7TM structure of GPCRs. Furthermore, for class A GPCRs such as $A_{2A}R$, allosteric binding sites are found near extracellular regions, making them accessible to solvents even more. For other classes of GPCRs, both orthosteric and allosteric binding sites can be found in either the center of the helix bundle or the extracellular loop region.[29]

Solvation effect inclusion: solvation energy re-scoring

From our analysis, it seems obvious that inclusion of the solvent effect in scoring of docking is beneficial. For this purpose, we tested a rescoring scheme in which implicit solvation energy is used to rescore poses generated and scored by Glide SP. The RMSD values of the redocking results produced with this scheme are shown in Table 2. The improvement when using this

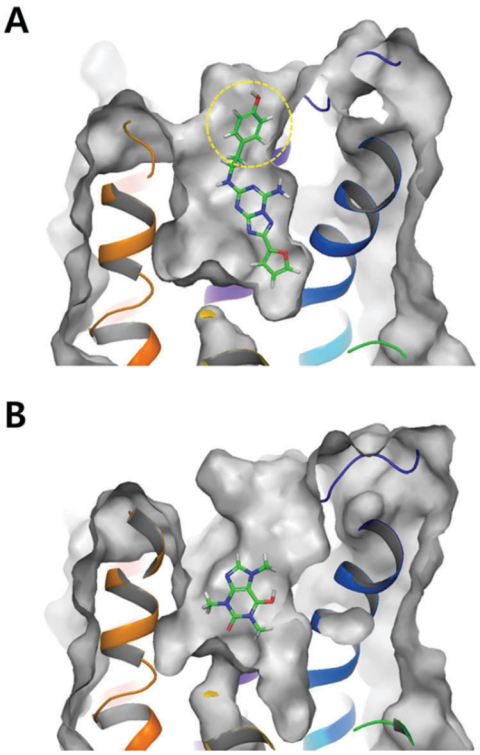

Fig. 2 Comparing two A2A adenosine receptor co-crystals in complex with ZM241385 and caffeine. (A) ZM241385–A2AR complex. Solvent exposed phenol group (yellow dotted circle) is located at the extracellular entrance of the binding site. (B) Caffeine–A2AR complex. Caffeine partially exposed to solvents although the whole ligand is located deep in the binding site.

rescoring scheme is incremental at best. Although all the success cases by Glide SP were not disrupted by the rescoring scheme, none of the failed cases by Glide SP were turned into success. The only notable case would be 4AMI, for which the RMSD value was reduced from 9.661 to 2.914, indicating that the predicted pose by inclusion of the solvent effect at least is in the correct orientation.

Polarization effect consideration

Compared with the membrane parts of GPCRs, solvent exposed surfaces, including extra-cellular loops, have relatively more polar and charged amino acids. Moreover, extra-cellular loop2 (ECL2) often participates in ligand interactions. Therefore, using correct atomic charges on atoms in this region for docking would be important. This means that one should incorporate polarization effects in some way. In a previous research of our group, we have shown that a docking protocol integrating DFT-based QM/MM calculations can be considerably effective for a wide range of targets.[23,30–32]

In that work, atomic charges on the ligand were recalculated using QM calculations and then used in docking instead of fixed charges coming from force field. In the current work, we employed the same procedure with extended QM regions. To see how much of difference these QM calculated charges can bring, we compared electrostatic energies between the ligands

Table 3 Ecvdw energies calculated by MM and QM/MM methods

	Ecvdw (kcal mol^{-1})	
PDB	MM	QM
2RH1	−45.23	−80.51
3D4S	−29.02	−62.95
3NY8	−31.30	−30.40
3NY9	−43.32	−92.80
3NYA	−26.81	−40.57
3SN6	−38.28	−68.40
4LDL	−46.75	−99.95
4LDO	−29.88	−62.93
2VT4	−42.76	−49.84
2Y00	−39.18	−55.70
2Y02	−55.00	−60.84
2Y03	−27.60	−37.51
2Y04	−32.02	−35.59
2YCW	147.46	−34.26
4AMI	−32.32	−41.96
3ZPQ	−29.75	−38.15
4AMJ	−61.97	−115.37
3EML	−35.70	−35.90
2YDO	−36.85	−38.93
2YDV	−54.18	−39.81
3REY	−29.70	−32.39
3RFM	−25.70	−20.30
3UZA	−12.50	−16.60
3UZC	−33.44	−28.50
3PBL	−29.30	−39.30
3RZE	−25.84	−36.71
4DAJ	−47.61	−82.88
4DJH	−45.00	−67.70
4EJ4	−37.02	−57.87
4EA3	−45.14	−105.07
3VW7	−66.96	−47.95
3UON	−46.85	−56.74
4MQS	−40.70	−38.14
4MQT	−44.06	−55.10
3V2W	−42.79	−59.37
4K5Y	−45.52	−51.31
4JKV	−71.86	−69.18
4IAR	−65.32	−99.63
4IAQ	−60.62	−75.41
4MBS	−60.58	−67.69

and the receptors calculated with both force field charges and QM charges at the native poses. In Glide, Ecvdw is the sum of Coulombic and van der Waals energies. However, in our protocol, by changing the charges, only electrostatic energies were affected, not van der Waals energies. The values of Ecvdw in both cases are listed in Table 3. As is evident from the table, Ecvdw values are significantly different in most cases; 23 cases over 10 kcal mol^{-1}. This means that polarization effects are substantial in the binding sites of GPCRs. Thus we applied QM/MM docking method described in ref. 23 and 27–29 for our test set.

The results of QM/MM docking on our test set are listed in Table 2. With QM/MM docking, the success rate was 90% with 1.12 Å RMSD average, which is significantly better than both regular Glide and solvent-included docking. QM/MM docking successfully predicted binding poses for 3RFM, 3UZA, 3PBL and 4DJH, which are cases with solvent exposed ligands. QM/MM docking still could not improve the binding pose prediction for 3EML, 3REY, 4AMI and 4MQT. From Table 3, one finds that Ecvdw values differ only by small amounts in cases of 3EML and 3REY. One can conclude, for these cases, that there is not much polarization effect that can be described by QM/MM calculations. For 4AMI and 4MQT, however, Ecvdw energies differ by substantial amounts. To explain why corrections of the polarization effect could not improve the binding pose prediction, we note that the ligands in these complexes have large portion of them exposed in the solvent. QM/MM calculations were performed for the protein without solvation by water and certainly would introduce errors in these cases. Inclusion of the solvent effect along with QM/MM calculations seems to be the inevitable next step.

Solvation QM/MM docking

The key concept of our new docking method for GPCR targets is in that ''environmentally accurate charges'' must be used in docking, by including both solvation and polarization effects (Fig. 3). Environmentally accurate charges are atomic charges deviating from force field parameters and conforming to the environment of solvent and polarizing residues.

We implemented our concept by QM/MM calculations with implicit solvent. In our implementation, which we dubbed ''solvation QM/MM docking'', QM regions include ligand atoms and surrounding residues in the binding site as described in the Method section.

A few previous studies have employed QM/MM-GB/SA (Generalized Born/Surface Area)[33,34] or QM/MM-PB/SA (Poisson–Boltzmann/Surface Area)[35] approaches to the bridge solvation model and QM/MM calculation in ligand docking. In these approaches, the solvation effect is incorporated by post-docking (re-scoring) treatment of GB/SA or PB/SA energy calculations. In contrast, our method takes into account solvation at the QM/MM energy calculation stage, which would give rise to more accurate atomic charges on ligands and binding site protein atoms and thereby provide better opportunities for finding accurate poses at the docking stage itself.

Our method was tested on the same GPCR docking assessment test set (Table 2). RMSD values for all the predicted binding poses were below 2 Å and the average was 0.776 Å.

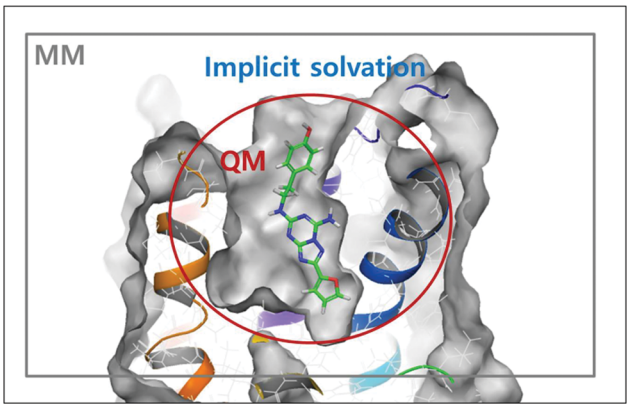

Fig. 3 Solvation QM/MM docking method for GPCR targets. The ligand atoms and the surrounding residues in the binding sites are described as the QM region and the rest as the MM region. The extracellular region is treated with the implicit solvent model.

For the failed cases using QM/MM docking without solvation, 3EML, 3REY, 4AMI and 4MQT, the RMSD values decreased from 6.335 to 0.546, from 3.996 to 1.223, from 2.924 to 0.489 and from 3.100 to 1.507, respectively. Solvation QM/MM docking made correct predictions for complexes in which the solvation effect can be important while retaining correct predictions made by Glide and QM/MM docking.

The 3EML docking result illustrates contribution of each of these effects well (Fig. 4). Glide docking resulted in a RMSD of 8.976 Å for 3EML. The predicted pose sits in the opposite direction of the native pose. QM/MM docking without solvation predicted the correct orientation of the ligand in the binding site with the core ring group and the furyl group in the same position as the native pose. One can conclude that having a set of better fitted atomic charges in this part of the ligand guided the orientation of the docking pose to the right direction. However, a deviation from the native pose was still present in the phenol group that is exposed to the solvent. Instead of pointing out to the extra-cellular region, the QM/MM docking-predicted pose had this functional group forming a hydrogen bond with His278. A RMSD of 6.355 Å for QM/MM docking was attributed to this error. Solvation QM/MM docking corrected this error and the RMSD value was greatly reduced to 0.546 Å.

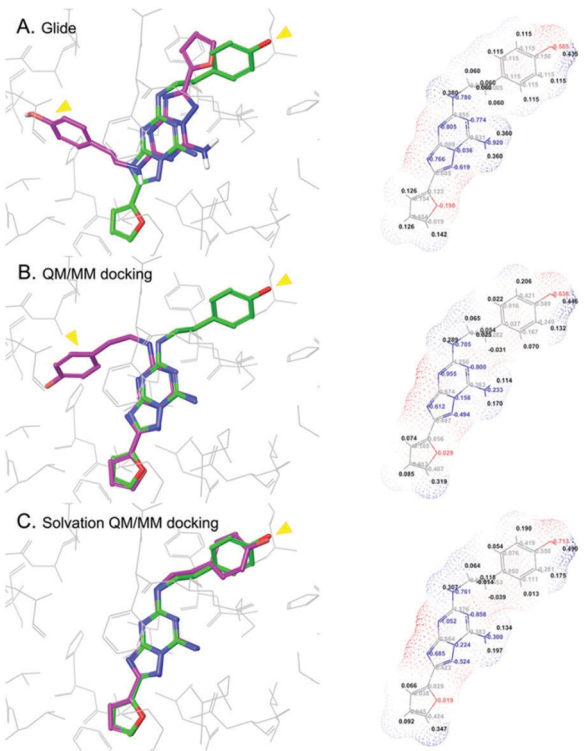

Fig. 4 Prediction of ZM241385 binding modes using the three docking methods and atomic charges of ligands (green – crystal pose, purple – predicted pose). Yellow triangle indicates the position of the phenol group. (A) Glide docking result and force field charges. (B) QM/MM docking result and ESP charges calculated by the QM/MM method. (C) Solvation QM/MM docking result and ESP charges calculated by the QM/MM method under an implicit solvent environment.

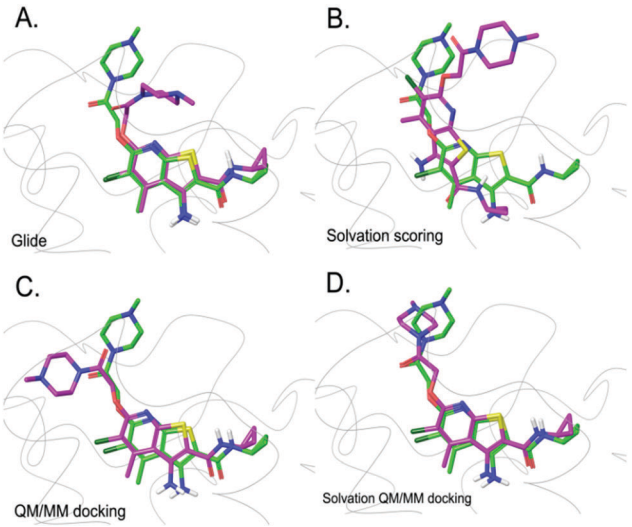

Fig. 5 Prediction of LY2119620 binding modes using the four docking methods (green – crystal pose, purple – predicted pose). (A) Glide docking result. (B) Solvation scoring result. (C) QM/MM docking result. (D) Solvation QM/MM docking result.

A similar explanation can be given to the case of 4MQT in which the binding site is an allosteric one near the solvent exposed ECL region (Fig. 5).

Successful predictions for these 2 cases strongly suggest that solvation QM/MM docking can be applied to GPCR targets of all classes encompassing different types of binding sites.

Gas phase QM docking

To demonstrate the importance of the environmental effect of the binding site protein atoms on polarization of ligand atoms, we performed QM calculations on ligands in the gas phase and followed the same protocol as QM/MM docking. The charges calculated in this way would reflect the self-polarization effect of the ligands coming from the molecular shape, but would miss the polarization effect exerted by the surrounding protein atoms. This protocol, which we named gas phase QM docking, showed slightly improved average RMSD as compared with Glide docking by only about 0.06 Å and in terms of the success rate, it actually had one more failure than Glide. Overall, gas phase QM docking could not match the performance of solvation QM/MM docking and this clearly shows that when taking into account polarizations of ligand atoms, the environmental influence must be considered.

A practical solvation QM/MM docking protocol

The above QM/MM docking studies were performed with native poses of crystal structures. In the field of real drug discovery, however, the docking method should be able to predict the binding mode of a novel ligand without a native pose. The SOF (survival of the fittest) algorithm[23] was developed for this purpose in the previous iteration of the QM/MM docking method. A similar algorithm was implemented for solvation QM/MM docking as described in the Method section. The protocol was called "SolvQMDock" and tested on the GPCR docking assessment set (Table 4).

Table 4 RMSD values (Å) of GPCR docking using SolvQMDock

	SolvQMDock
PDB	RMSD (Å)
2RH1	0.908
3D4S	1.073
3NY8	1.040
3NY9	0.911
3NYA	0.909
3SN6	1.425
4LDL	1.454
4LDO	0.363
2VT4	0.526
2Y00	0.699
2Y02	1.795
2Y03	0.562
2Y04	0.598
2YCW	0.705
4AMI	0.494
3ZPQ	0.408
4AMJ	1.982
3EML	0.563
2YDO	0.958
2YDV	0.190
3REY	1.243
3RFM	0.772
3UZA	1.229
3UZC	1.705
3PBL	0.755
3RZE	0.745
4DAJ	1.670
4DJH	0.894
4EJ4	0.853
4EA3	1.727
3VW7	0.529
3UON	0.526
4MQS	2.173
4MQT	1.492
3V2W	0.504
4K5Y	0.488
4JKV	1.974
4IAR	0.328
4IAQ	0.360
4MBS	2.190
Average	0.993
Range	0.190–2.190
Success rate	38/40

10 ligand poses generated during the process of SolvQMDock cover a wide range of ligand RMSD values and the charge values on them calculated by the solvation QM/MM method varied accordingly. An example of 3REY is shown in the ESI,† S2. It should also be noted that the implicit solvation energy calculated on these intermediate poses would also vary, but this effect is infused in the charge values. Some of the charge values may seem to be unrealistic but one must keep in mind that it is the electrostatic potential surface that eventually matters. In SolvQMDock, a second round of docking is performed with these charge values; therefore, both polarization and solvation effects are counted in search of correct poses. In comparison with the results of solvation QM/MM docking with native ligands, the average RMSD value by SolvQMDock slightly increased from 0.776 Å. However, the new method still performed better on GPCR targets than Glide docking, which exhibited an average RMSD of 1.735 Å. For 2 GPCR complexes (4MQS and 4MBS), our protocol showed RMSD values of more than 2 Å. In both cases, the failure came from the prediction of the ring conformation while the general orientation of the whole ligand was correct (Fig. 6). Except for these 2 cases, SolvQMDock displayed accurate docking prediction capabilities in an actual drug discovery environment.

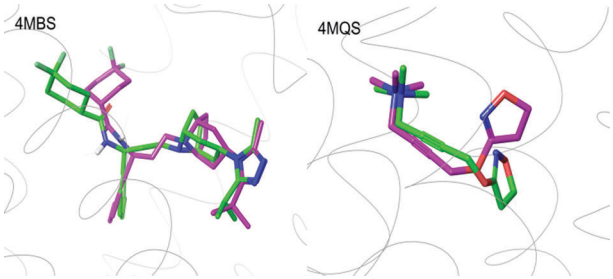

Fig. 6 Docked poses for 4MBS and 4MQS (green – crystal pose, purple – predicted pose).

SolvQMDock can be computationally demanding as it includes QM calculations on regions that encompass some of protein atoms in the binding sites as well as ligand atoms. Solvation phase QM/MM calculations further exacerbate the situation as QM calculations in solvation take twice as much as those in the gas phase. For a typical GPCR complex, solvation QM/MM docking calculation took about 7 hours on the single Intel® Xeon X5650 @ 2.67GHz processor. Parallelization by ligand poses generated before the QM/MM calculation stage would cut this time nearly 10 fold; however, the protocol is probably suitable for the lead optimization process rather than virtual ligand screening.

Conclusions

In this work, we have presented a docking strategy which combines QM/MM calculation with the implicit solvent model. The main aim of our approach was to propose a new docking method which performs with high reliability and accuracy for GPCR targets. Since most GPCRs have solvent accessible binding sites as we have identified, inclusion of solvation and polarization effects was expected to improve the docking performance on GPCR targets. Our implementation involved reparametrization of partial charges on atoms of the ligands and the side chains in the proximity of binding sites using QM/MM calculations along with solvation energy calculations using the implicit solvent model.

As a proof-of-concept, the docking accuracy test on a set of 40 GPCR complexes was carried out to compare 4 methods (Glide SP, solvation energy rescoring, QM/MM docking with native poses, and solvation QM/MM docking with native poses). In this test, the solvation energy rescoring method did slightly better than the conventional docking program, Glide. QM/MM docking, on the other hand, did much better, succeeding in 90% of cases as opposed to 80% for Glide. Those failed cases with QM/MM docking were analyzed and it was observed that solvent exposed parts were predicted to be in wrong conformations. Solvation QM/MM docking corrected this error and the

success rate turned out to be 100%. Our results strongly suggest that incorporating polarization and solvent effects in docking certainly benefits for GPCR targets of all classes and all types of binding sites.

However, in order to utilize the solvation QM/MM docking method in an actual drug discovery environment, one needs an algorithm which does not require knowledge of native poses. For this purpose, we incorporated the SOF algorithm with solvation QM/MM docking and coined the resulting protocol as SolvQMDock. It was tested on the same set of GPCR complexes. The success rate of this test was 95%, which is high enough a number for the new docking protocol to be used for GPCR targets reliably.

Acknowledgements

This work was supported by the National Research Foundation of Korea (no. 2013R1A2A2A01067638, 2012M3C1A6035362, and 2016M3A7B4025405). We thank Schrödinger, LLC, for the provision of its software for our research.

References

1 T. K. Bjarnadottir, D. E. Gloriam, S. H. Hellstrand, H. Kristiansson, R. Fredriksson and H. B. Schioth, *Genomics*, 2006, **88**, 263–273.
2 D. Filmore, *Mod. Drug Discovery*, 2004, **7**, 24–28.
3 M. C. Lagerstrom and H. B. Schioth, *Nat. Rev. Drug Discovery*, 2008, **7**, 542.
4 J. P. Overington, B. Al-Lazikani and A. L. Hopkins, *Nat. Rev. Drug Discovery*, 2006, **5**, 993–996.
5 R. Lappano and M. Maggiolini, *Nat. Rev. Drug Discovery*, 2011, **10**, 47–60.
6 I. Kufareva, V. Katritch, R. C. Stevens and R. Abagyan, *Structure*, 2014, **22**, 1120–1139.
7 M. Congreve, C. J. Langmead, J. S. Mason and F. H. Marshall, *J. Med. Chem.*, 2011, **54**, 4283–4311.
8 A. C. Anderson, *Chem. Biol.*, 2003, **10**, 787–797.
9 T. Lengauer and M. Rarey, *Curr. Opin. Struct. Biol.*, 1996, **6**, 402–406.
10 T. Beuming and W. Sherman, *J. Chem. Inf. Model.*, 2012, **52**, 3263–3277.
11 V. Katritch, V. P. Jaakola, J. R. Lane, J. Lin, A. P. IJzerman, M. Yeager, I. Kufareva, R. C. Stevens and R. Abagyan, *J. Med. Chem.*, 2010, **53**, 1799–1809.
12 L. T. May, K. Leach, P. M. Sexton and A. Christopoulos, *Annu. Rev. Pharmacol. Toxicol.*, 2007, **47**, 1–51.
13 A. C. Kruse, A. M. Ring, A. Manglik, J. X. Hu, K. Hu, K. Eitel, H. Hubner, E. Pardon, C. Valant, P. M. Sexton, A. Christopoulos, C. C. Felder, P. Gmeiner, J. Steyaert, W. I. Weis, K. C. Garcia, J. Wess and B. K. Kobilka, *Nature*, 2013, **504**, 101–106.
14 K. S. Watts, P. Dalal, R. B. Murphy, W. Sherman, R. A. Friesner and J. C. Shelley, *J. Chem. Inf. Model.*, 2010, **50**, 534–546.
15 *Protein Preparation Wizard*, Schrödinger, LLC, New York, NY, 2014.
16 M. H. M. Olsson, C. R. Sondergaard, M. Rostkowski and J. H. Jensen, *J. Chem. Theory Comput.*, 2011, **7**, 525–537.
17 *Protein Assignment utility*, Schrödinger, LLC, New York, NY, 2014.
18 *Prime, version 3.8*, Schrödinger, LLC, New York, NY, 2014.
19 *version 6.5*, Schrödinger, LLC, New York, NY, 2014.
20 R. A. Friesner, J. L. Banks, R. B. Murphy, T. A. Halgren, J. J. Klicic, D. T. Mainz, M. P. Repasky, E. H. Knoll, M. Shelley, J. K. Perry, D. E. Shaw, P. Francis and P. S. Shenkin, *J. Med. Chem.*, 2004, **47**, 1739–1749.
21 T. A. Halgren, R. B. Murphy, R. A. Friesner, H. S. Beard, L. L. Frye, W. T. Pollard and J. L. Banks, *J. Med. Chem.*, 2004, **47**, 1750–1759.
22 *MacroModel, version 10.6*, Schrödinger, LLC, New York, NY, 2014.
23 A. E. Cho, V. Guallar, B. J. Berne and R. Friesner, *J. Comput. Chem.*, 2005, **26**, 915–931.
24 *QSite, version 6.5*, Schrödinger, LLC, New York, NY, 2014.
25 *Jaguar, version 8.6*, Schrödinger, LLC, New York, NY, 2014.
26 D. Bakowies and W. Thiel, *J. Phys. Chem.*, 1996, **100**, 10580–10594.
27 H. Lin and D. G. Truhlar, *Theor. Chem. Acc.*, 2007, **117**, 185–199.
28 S. Pezeshki and H. Lin, *Mol. Simul.*, 2015, **41**, 168–189.
29 P. J. Conn, A. Christopoulos and C. W. Lindsley, *Nat. Rev. Drug Discovery*, 2009, **8**, 41–54.
30 J. Y. Chung, J. M. Hah and A. E. Cho, *J. Chem. Inf. Model.*, 2009, **49**, 2382–2387.
31 A. E. Cho and D. Rinaldo, *J. Comput. Chem.*, 2009, **30**, 2609–2616.
32 A. E. Cho, J. Y. Chung, M. Kim and K. Park, *J. Chem. Phys.*, 2009, **131**, 134108.
33 K. Wichapong, A. Rohe, C. Platzer, I. Slynko, F. Erdmann, M. Schmidt and W. Sippl, *J. Chem. Inf. Model.*, 2014, **54**, 881–893.
34 P. C. Su, C. C. Tsai, S. Mehboob, K. E. Hevener and M. E. Johnson, *J. Comput. Chem.*, 2015, **36**, 1859–1873.
35 S. A. Hayik, N. Liao and K. M. Merz, *J. Chem. Theory Comput.*, 2008, **4**, 1200–1207.